Image Correlation to Evaluate the Influence of Hygrothermal Loading on Wood

Cécilia Gauvin (a), Delphine Jullien (a),
Pascal Doumalin (b), Jean-Christophe Dupré (b), Joseph Gril (a)
(a) Laboratory of Mechanical and Civil Engineering,
UMR5508, CNRS, University of Montpellier 2
(b) Institut Pprime, UPR 3346, CNRS, University of Poitiers

March 10, 2016

1 Introduction

Many wooden objects from cultural heritage consist in wooden panels, painted on one face. Nowadays some of these panels show permanent cupping, microcracks of the paint layer, cracks of the wooden support itself. Different physical and mechanical phenomena are at the origin of these damages: wood is a hygroscopic material (its dimensions vary with humidity), it is highly anisotropic, the paint layer on one face has properties of permeability different from raw wood of the back face, a rigid frame possibly restrained the deformation of the panel.

The mechanical engineer may contribute to the conservation issue by giving expertise on a given artwork or collection, such as acceptable microclimatic conditions, the risk associated to the movement of the object, the opportunity to modify the frame. A numerical modelling of painted panels has been developed in LMGC these last years [1], [2]. It is based on *in-situ* data collected on instrumented panels. We now need to collect a set of data concerning both the behaviour of an equivalent material and the reaction of a panel constituted by this well-identified material and submitted to controlled hygrothermal fluctuations. Experimentations on our mock-up panels combined numerical simulations of these panels in real situations of hygrothermal fluctuations will allow us to test specific situations and eventually to make suggestions to conservators and restorers and guide them in their interventions.

For this purpose, we tried to develop a non-invasive tool which can give us a full field measurement. Digital image correlation (DIC) is a powerfull technique to get displacement and strain field on material surfaces [3]-[9].

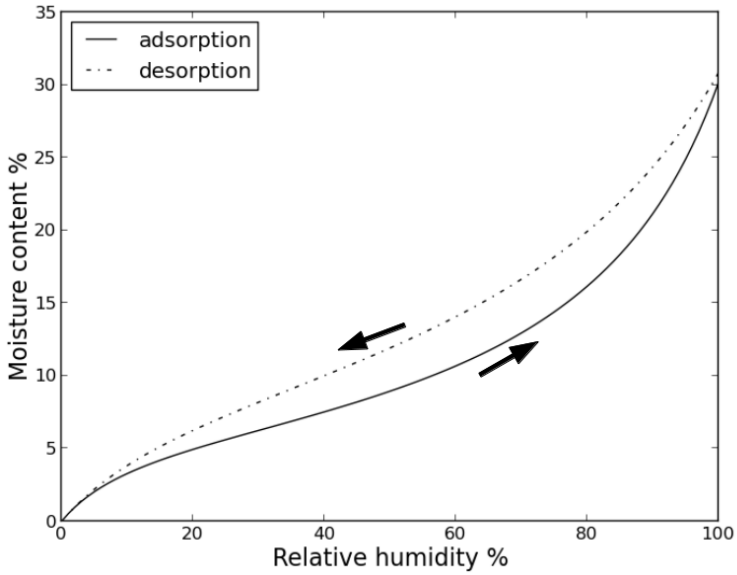

Figure 1: *Sorption Isotherm in Wood. Based on data from [12].*

This technique has also been developped for anisotropic material such as wood [10], [11]. For our case, we tried to adapt DIC for cultural heritage aim, *i.e.* to follow during several weeks or years the same object. It is not the usual use of that technique, normally performed with short periods allowing a fixed setting of the equipment.
This paper shows simple cases of loading on wood (submitted to variations of relative humidity) to ensure that we can evaluate correctly the deformation field with several manipulations of the specimens. Two experiments were performed, one with a simple change of relative humidity to confirm the anisotropic properties of wood and another one with cycling change of relative humidity to observe the effect of a loss of hygroscopicity.

2 Material and methods

2.1 Water in wood

Wood is sensitive to atmospheric climate, relative humitidy and temperature. Its moisture content (mass of water divided by ovendry mass) changes with the environment and, for a given climate, tends to a stable state called equilibrium moisture content. For the same relative humidity and temperature, the moisture content is not the same if the wooden specimen is in adsorption (of water) or desorption stage. This is due to the hysteresis behaviour as shown in Figure 1.

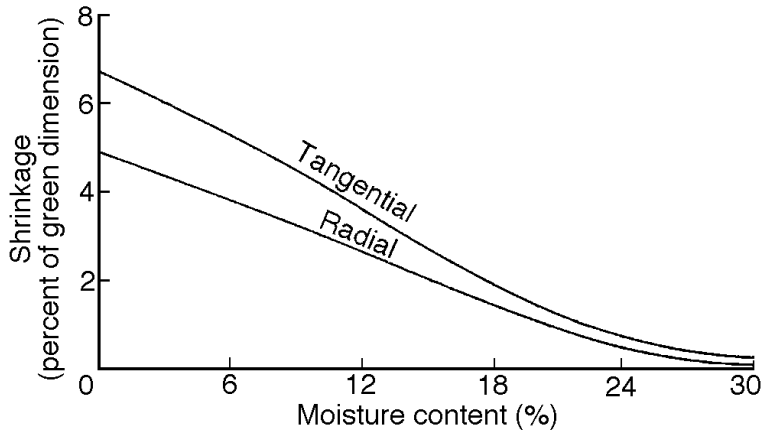

Figure 2: *Typical shrinkage vs moisture content curves [14].*

In green state, for example in standing tree, wood is full of water: its moisture content may exceed 100%. When wood dries, "free" water is released first without any change of dimension, down to the fiber saturation point (typically 30%). Below that, "bound" water is released, accompanied with anisotropic shrinkage proportional to water loss (Figure 2).

Material density depends on the position in the log relatively to the pith: wood is made of a succession of concentric layers, alternating lighter and denser material (respectively earlywood and latewood). Three orthotropic directions are commonly defined: longitudinal (**L**), along fiber direction, radial (**R**), perpendicular to rings and tangential (**T**), tangential to rings (Figure 3).

The anatomical and ultrastructural organization of wood leads to a high anisotropy. Moisture-induced expansion (swelling or shrinkage) is less than 0.1% in **L** direction, and about twice higher in **T** than in **R** directions (Figure 4), typically between 8 % and 5 %, respectively for poplar wood - between saturated and ovendry state [14]. Moreover, due to this anisotropy, the diffusion inside wood is quite different depending the direction of interest. The diffusion in **L** direction is 10 times more than in **T** or **R** directions [15]. To quantify these phenomena, weight and dimensions were measured on wood samples, stabilized at different humidities.

2.2 Material

The species used is poplar (*Populus Alba*). Two kinds of board were used: a flatsawn board and a quartersawn board (Figure 5).

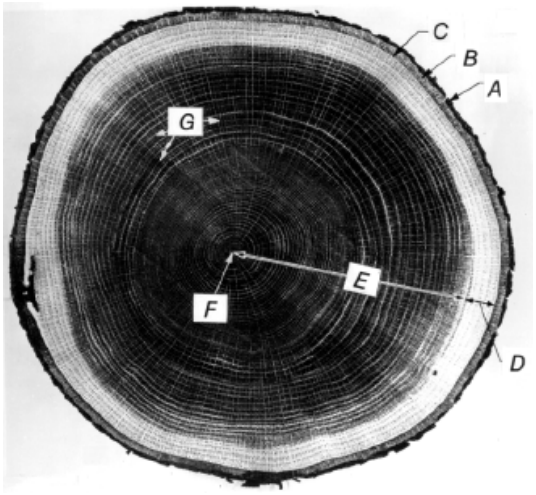

Figure 3: *Cross Section of a trunk:* ***(A)*** *outer bark,* ***(B)*** *inner bark,* ***(C)*** *cambium (production of wood and bark),* ***(D)*** *sapwood,* ***(E)*** *heartwood,* ***(F)*** *pith, and* ***(G)*** *ring = (earlywood + latewood) [13].*

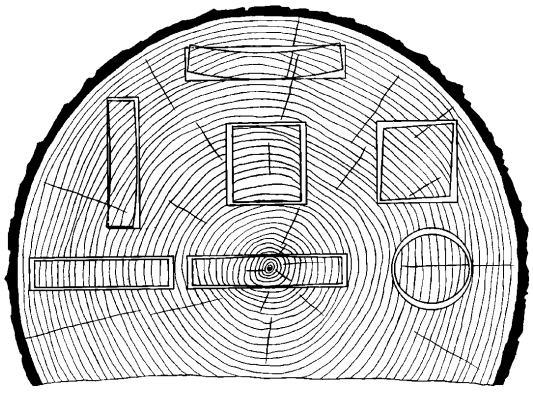

Figure 4: *Shrinkage and distortion of flat, square, and round pieces are affected by direction of growth rings. Tangential shrinkage is about twice as great as radial one [14].*

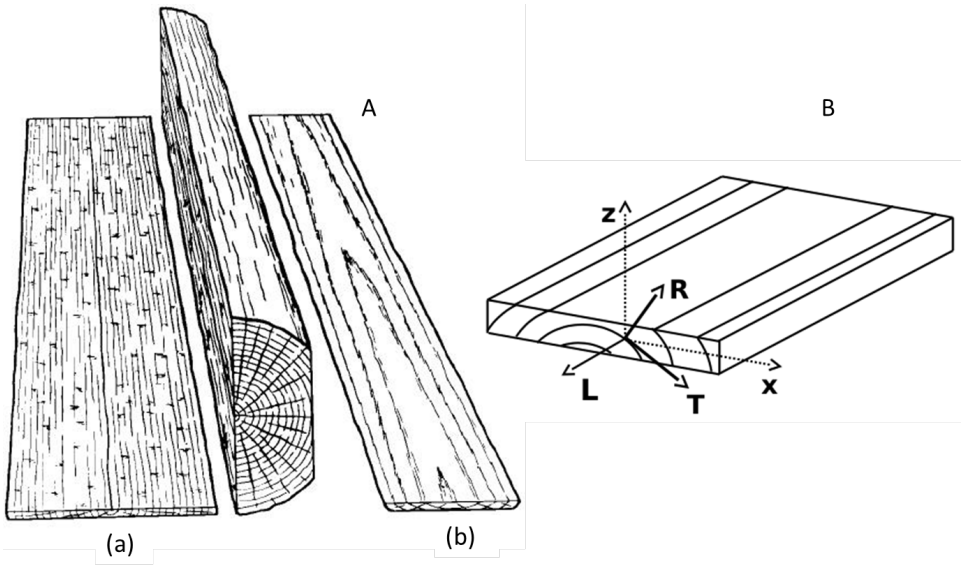

Figure 5: *Specimen types. Boards from a log* ***(A)****: Quartersawn* ***(a)*** *and flatsawn* ***(b)*** *boards cut from a log [14]. Orthotropic orientation* ***(B)****: Wood panel [2].*

Two sets of specimens were used:

set (1): In order to analyze if the annual rings influence the speckle and consequently the displacement field, two kinds of coating were used: one transparent, rubber, and one opaque, Dipetanch©.
Dimensions of specimen are T=290 x L=6 x R=40 mm^3 for flatsawn and R=210 x L=10 x T=27 mm^3 for quartersawn (Figure 6). We applied waterproof coating on 4 faces of sample to force the diffusion in a preferential direction: **R** in the case of flatsawn boards, **T** in the case of quatersawn boards.

set (2): Dimensions of specimens are T=290 x L=10 x R=40 mm^3 for flatsawn and R=210 x L=10 x T=27 mm^3 for quartersawn. We applied rubber coating on different faces to control the preferential hydration orientation of our samples. Here, we focus on situations involving diffusion along the **L** direction of the samples.
We applied on this set of sample a hygrothermal loading using hygroscopic cycles.

A climatic chamber is used to control temperature and relative humidity environment, with a precision of ± 3 °C and ± 3 %RH.

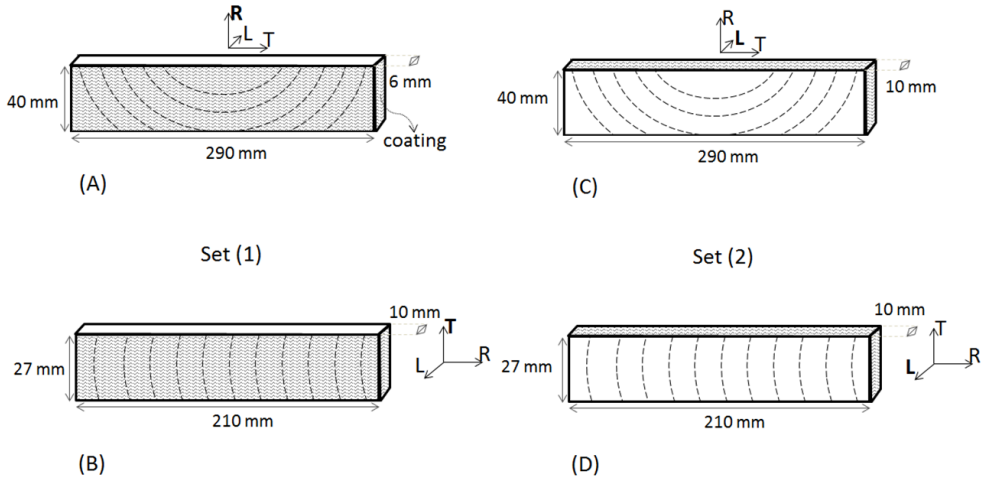

Figure 6: *Specimen sizes. Grey color corresponds to coated faces.* ***(A)*** *set (1) Flatsawn,* ***R*** *diffusion.* ***(B)*** *Quartersawn set (1),* ***T*** *diffusion.* ***(C)*** *set (2) Flatsawn,* ***L*** *diffusion.* ***(D)*** *Quartersawn set (2),* ***L*** *diffusion.*

2.3 Hygroscopic variations and humidity cycles

Painted panels have been generally submitted to variable humidity environment during centuries. To evaluate the effect of such a loading, we conducted tests with drastic changes of humidity during some days or weeks, that may be comparable to softer cycles during long period. Accelerating procedure is often used in wood ageing studies [16], [17].

For set (1), samples were first stabilized at 75% RH, 20°C then humidified up to 90% RH, 20°C until their mass equilibrium (Figure 7).

Then, to test the effect of hygrothermal loading: eleven 36-hours-long humidity cycles (Figure 8) were imposed between 40% and 90% RH, at 50 °C to specimens from set (2) (Figure 6). The hygroscopic response was simulated using Transpore [18], [19], a wood drying simulator, which indicated that the equilibrium moisture content of our 10 mm width specimens (**L** diffusion orientation) was reached with a 15 hours plateau.
Pictures were taken at different times (T1...T9) during cycles, at the end of plateau to be sure that samples were at the equilibrium moisture content.

2.4 Full-field measurement: Digital Image Correlation

We used DIC to measure the strain field induced by our hygroscopic treatment. A 2D analysis was perfomed because the out-of-plane deformations are negligible [20], [21] in this configuration.

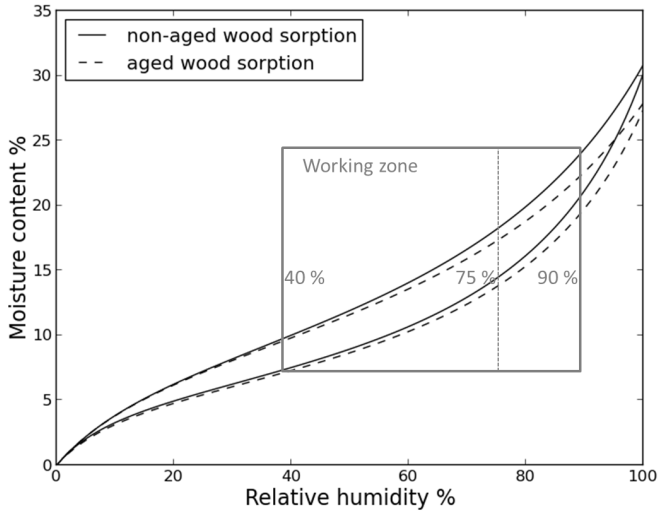

Figure 7: *Sorption isotherm of "non-aged" wood and "aged" wood. Inspired by [16].*

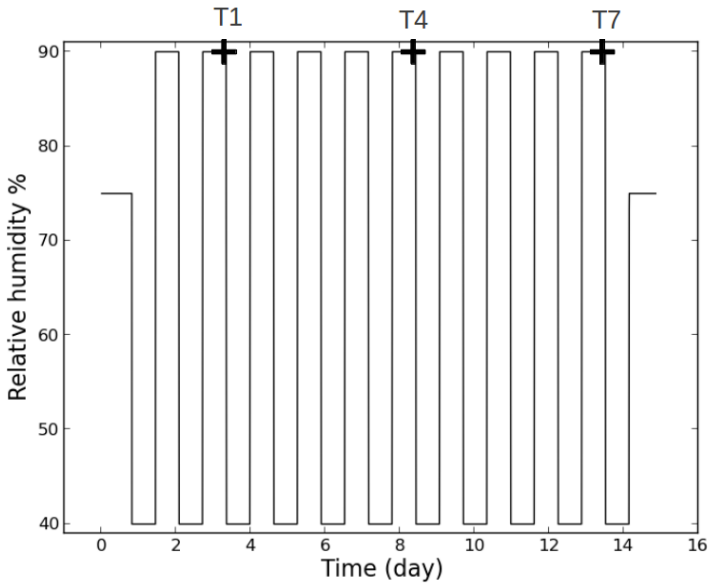

Figure 8: *Hygroscopic cycles.*

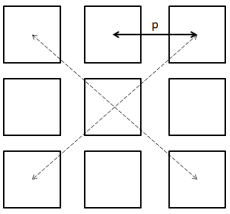

Figure 9: *Calculation for four subsets incross. p is the distance between two subsets.*

Pictures are taken using a color camera (Canon EOS 600D©) with a 60 mm, f/2.8 lens. The spatial resolution of images is 0.0634 mm/pixel. This kind of camera was used because of its high resolution. Unfortunately the fill factor of the pixels, less than one (due to the principle of a tri-cmos color captor) decreases the accuracy. The color pictures are transformed to grey level images to be used by DIC.
For each test, the specimens had to be taken out of the chamber imposing the climate treatment. The duration of the weighting and optical observation (less than 3 min) was short enough to have no significant effect on the moisture distribution in the specimen. To ensure that each time the specimen was at the same position, we prepared cyclindric block references to guide it during the observation. Although the rigid body displacements are eliminated by the gradient operator used to calculate strains, this technique of sample re-placement allows the 2D-analysis to be done. Since we can not follow continuously the samples during the cycles, the analysis would loose the displacement of the pattern in case of a too large displacement.
Using CORRELA2012 (home-made sofware developped by the team PEM of Institut PPRIME [3]) [1], we calculated the corresponding deformation field. Concerning the correlation process, we used a regular grid of subsets sized as 64x64 pixel^2 and placed with a 16-pixels interval in the two directions and a step of 2 for all of the specimens. We use also the least-squares method to find the best matching between two homologous subsets and material transformation assumed in DIC process as a translation and a local homologous gradient. A bilinear interpolation of grey levels is performed on images to achieve subpixel values of displacement.
The deformations are calculated by finite differences [22] from a cross as defined in Figure 9.

Two pictures at the same state are used to assess the accuracy in deformation. The maximal value of strains ϵ_{max} found by DIC gives a measurement uncertainty equal to 0.1%. This corresponds to a displacement uncertainty close to $8\mu m$ according to the following formula :

[1] http://www.pprime.fr/?q=en/photomechanics

$\epsilon_{max} = \frac{\Delta U}{8p}$
with ΔU the uncertainty of displacement at each subset, p the distance between two subsets and the finite difference scheme chosen as shown in Figure 9). So the accuracy is enough for our case to observe strains between 0.2 and 5%.

The reference picture corresponds, in both cases, to an equilibrium state at 75 % RH, 50°C before treatment.

3 Results and discussion

3.1 Year-ring influence on strain distribution

Figures 10 and 11 compare the strain distribution with both speckles and annual rings (transparent rubber, dashed line) and with speckles only (opaque Dipetanch©, solid line). On both figures latewood/earlywood transitions are indicated with dotted line. We can see in Figure 10 that:

- The strain intensity is consistent with the ring shape: pixel positions on the strain of the central section profil **(C)** are consistent with the natural pattern of wood**(B)**;
- ϵ_{xx}, which corresponds to **T** strain in the central section of the specimen, does not change much with radial position;
- ϵ_{yy}, which corresponds to **R** strain in the central section of the specimen, varies within rings: swelling is clearly higher (almost twice) in latewood than in earlywood**(A)**, such as [11]. This observation is in good agreement with the known fact that the denser the wood, the higher the swelling [23].
- The specimen coated with Dipetanch© (solid line in (C)) is less deformed than the rubber-coating specimen (dashed line). The peaks occur quite at the same y-position for both.

Figure 11 is similar to Figure 10, showing results on quatersawn boards. Here, ϵ_{xx}, corresponding to radial strain, is about twice less, on the average, than tangential strain (ϵ_{yy}), a typical result for wood shrinkage or swelling. Moreover, concerning the different coatings, rubber-coating specimen is less constrained than the Dipetanch©-coating specimen. We can interprete this result as an effect of rigidification of the Dipetanch© face by the coating.

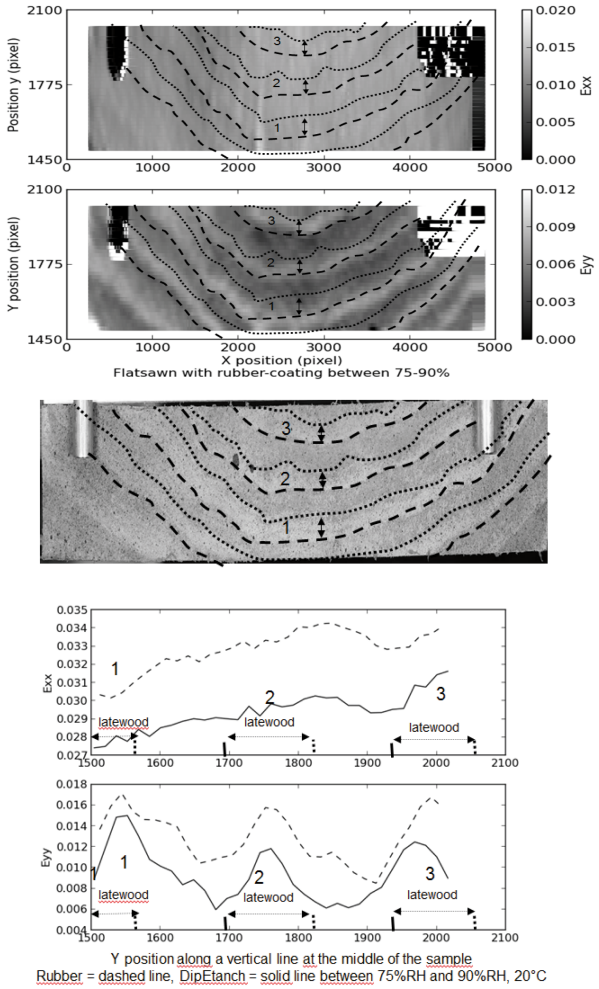

Figure 10: *Strain distribution on a flatsawn sample humidified from 75% to 90% RH.* ***(A)*** *Result from image analysis with CORRELA2012.* ***(B)*** *Growth ring situation compared to the result in (A).* ***(C)*** *Deformation profile along a vertical line at the middle of the sample.*

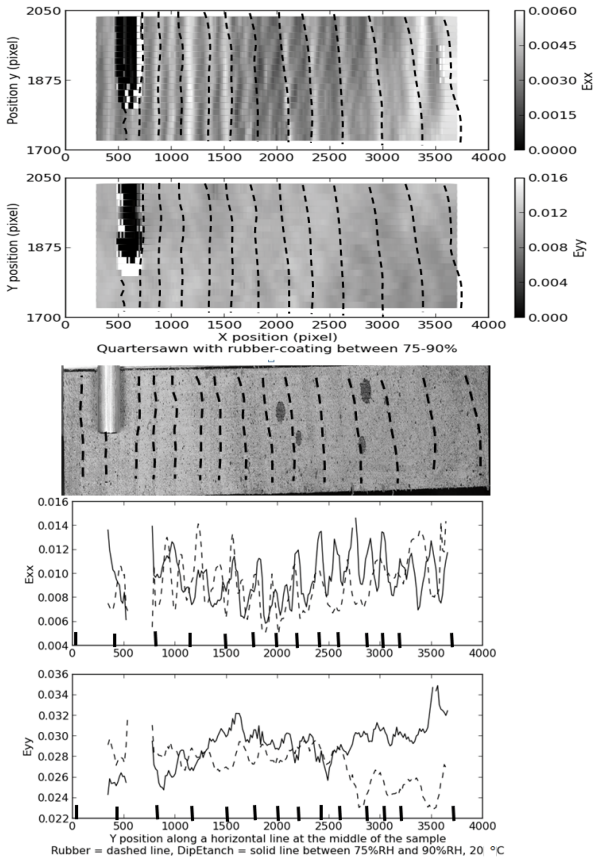

Figure 11: *Strain distribution on a quatersawn sample between 75 % and 90 % RH.* ***(A)*** *Result from image analysis with CORRELA2012.* ***(B)*** *Growth ring situation compared to the the result in (A).* ***(C)*** *Deformation profile along a horizontal line at the middle of the sample.*

We based our model to study painted panel at a macroscale level [1],[2], considering a homogeneous structure. But in fact, wood presents a strong heterogeneity between earlywood and latewood. This can disturb the painted layer. With this technique we can reach the response due to the heterogeneity.

3.2 Effect of hygrothermal loading

The 90 % RH flatsawn data (Figure 12) show that ϵ_{xx} and ϵ_{yy} deformations decreased with cycles: the hygroscopic ageing may induce a reduction of swelling. The same result is found for the quartersawn sample (Figure 13).

This decrease of deformation suggests that the samples loose hygroscopicity. Cycles of hygroscopic variations may introduce a so-called "chemical ageing" of the cell walls, leading to a loss of polarity [24],[16]: for the same relative humidity, cell walls adsorb less water after cycles than before, the equilibrium moisture content is lower after cycles. This chemical ageing would influence the isotherm curve (Figure 7). We expect that an "aged" wood, that has been subjected to many humidity cycles, is more dimensionally stable than a "non-aged" wood, more sensitive to changes of humidity.

ϵ_{xx} and ϵ_{yy} strain fields include radial and tangential strain components. The higher deformation of ϵ_{xx} located around 2000 pixels on X axis (Figure 12) is explained by the concordance of the **X** and the **T** directions in this area.

4 Conclusion

To conclude, we have measured the dimensional variations of wood samples submitted to hygrothermal cycles by Digital Image Correlation. The results have evidenced a loss of hygroscopicity of wood after cycles. This phenomenon could be attributed to chemical ageing. The strain fields obtained by DIC are in very good agreement with the anisotropic behaviour expected after macroscopic observations such as the position and the orientation of growth rings. This method allows us to evidence the higher swelling of latewood compared to earlywood.
Moreover, these experiments are the begining of our general aim, that is to set up tools for restorers and curators. We have verified that DIC technique is convenient for our purpose, considering the accuracy and the anisotropic properties we measured. But we did not make a quantitative study because of the anisotropic structure. We have to be careful about the position of the subset during the calculation, to do not smooth between latewood and

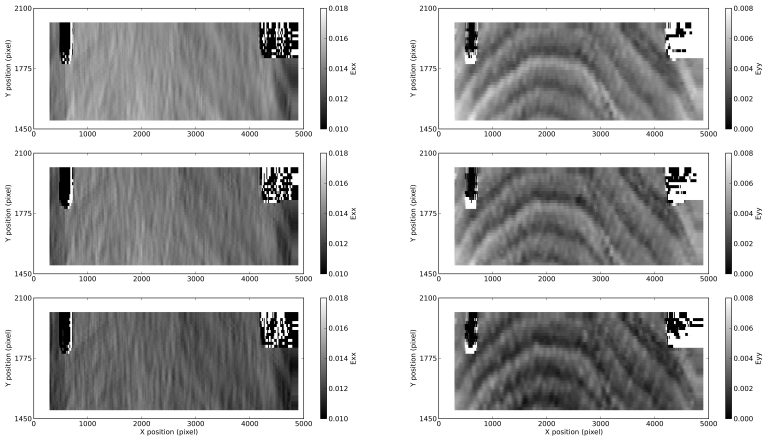

Figure 12: *Hygrothermal loading. Strain evolution of poplar flatsawn sample at 90% RH (compared to 75% RH), 50 °C.* ***A****: time T1, after 1 humidity cycle.* ***B****: at time T4, after 5 humidity cycles.* ***C****: at time T7, after 9 humidity cycles.*

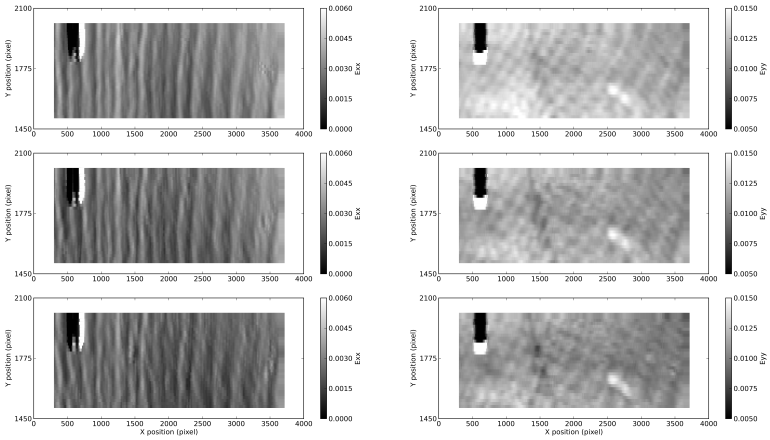

Figure 13: *Hygrothermal loading. Strain evolution of poplar quatersawn sample at 90% RH (compare to 75% RH), 50 °C.* ***A****: time T1, after 1 humidity cycle.* ***B****: at time T4, after 5 humidity cycles.* ***C****: at time T7, after 9 humidity cycles.*

earlywood. If we focus on that point, we can develop this method to quantitative results.
Now we have to adapt our method to the case of a panel mock-up where significant out-of-plane movements are expected.

References

[1] Marcon, B. *Hygromécanique des panneaux en bois et conservation du patrimoine culturel.* (in french) PhD, Université Montpellier 2, Università degli studi di Firenze. (2009).

[2] Colmars, J. *Hygromécanique du matériau bois appliquée à la conservation du patrimoine culturel : Étude sur la courbure des panneaux peints.* (in french) PhD, Université de Montpellier 2. (2011).

[3] Barranger, Y., Doumalin, P., Dupré, J. C. and Germaneau, A. *Strain Measurement by Digital Image Correlation: Influence of Two Types of Speckle Patterns Made from Rigid or Deformable Marks.* Strain: 48, 357-365. (2012).

[4] Bruck, H. A., McNeill, S. R., Sutton, M. A. and Peters, W. H. *Digital correlation using Newton-Raphson method of partial differential correction.* Experimental Mechanics, 29: 261-267. (1989).

[5] Choi, S. and Shah, S. P. *Measurement of deformations on concrete subjected to compression using image correlation.* Experimental Mechanics, 37: 307-313. (1997).

[6] Chu, T.C., Ranson, W.F., Sutton, M.A. and Peters, W.H. *Application of digital image correlation techniques to experimental mechanics.* Experimental Mechanics (1985): 232-244. (1985).

[7] Lu, H. and Cary, P. D. *Deformation measurements by digital image correlation: implementation of a second-order displacement gradient.* Experimental Mechanics, 40: 393-400. (2000).

[8] Tong, W. *An evaluation of digital image correlation criteria for strain mapping applications.* Strain 41, 167-175. (2005).

[9] Vendroux, G. and Knauss, W. G. *Submicron deformation filed measurements: part 2. Improved digital image correlation.* Experimental Mechanics, 38: 86-92. (1998).

[10] Choi, D., Thorpe, J.L., Hanna, R. B. *Image analysis to measure strain in wood and paper.* Wood Science Technology, Issue 25, 251-262. (1991).

[11] Jernkvist, L.O. and Thuvander, F. *Experimental Determination of Stiffness Variation Across Growth Rings in Picea abies.* Holzforschung, Issue 55, 309-317. (2001).

[12] Ahlgren, L. *Fuktfixering i porosa byggnadsmaterial (Moisture fixation in porous building materials).* Report 36, Division of Building Technology, The Lund Institute of Technology. (1972).

[13] Miller, R. B. *Structure of Wood.* Wood handbook. Wood as an engineering material. Forest Products Laboratory, United States Department of Agriculture Forest Service, Madison. Chapter 2. (2010).

[14] Simpson, W. and TenWolde, A. *Physical Properties and Moisture Relations of Wood.* Wood handbook. Wood as an engineering material. Forest Products Laboratory, United States Department of Agriculture Forest Service, Madison. Chapter 3. (2010).

[15] Siau, J. F. *Transport processes in wood. Springer series in Wood Science.* Springer-Verlag. (1984).

[16] Esteban, L.G., Gril, J., De Palacios De Palacios, P. and Guindeo Casasús, A. *Reduction of wood hygroscopicity and associated dimensional response by repeated humidity cycles.* Annals of Forest Sciences, Volume 62, Number 3, 275 - 284. (2005).

[17] Obataya, E. *Characteristics of aged wood and Japanese traditional coating technology for wood protection.* Actes de la journée d étude Conserver aujourdâhui : les "vieillissements" du bois. Cité de la Musique. (2007).

[18] Perre, P. *Fundamentals of Wood Drying.* European COST. A.R.BO.LOR. (2007).

[19] Rémond, R. *Approche déterministe du séchage des avivés de résineux de forte épaisseur pour proposer des conduites industrielles adaptées.* (in french) PhD, École Nationale du Génie Rural des Eaux et des Forêts, Centre de Nancy. (2004).

[20] Green, D. W., Winandy, J. E. and Kretschmann D. E. *Mechanical Properties of Wood.* Wood handbook. Wood as an engineering material. Forest Products Laboratory, United States Department of Agriculture Forest Service, Madison. Chapter 4. (2010).

[21] Guitard, D. *Mécanique du matériau bois et composites.* (in french) Cepadues Editions. Nabla Collection. (1987).

[22] Bretagne, N., Valle, V. and Dupré, J.C. *Development of the marks tracking technique for strain field and volume variation measurements.* NDTE International 5: 1-9. (2004).

[23] Time, B. *Hygroscopic Moisture Transport in Wood.* PhD, Norwegian University of Science and Technology, Department of Building and Construction Engineering. (1998).

[24] Skaar, C. *Wood-Water Relations.* Springer Series in Wood Science. Springer- Verlag, Berlin Heidelberg, pp. 283. (1988).